

LETTER

Photomineralization of organic carbon in a eutrophic, semiarid estuaryHongjie Wang ^{1*}, Xinping Hu ¹, Michael S. Wetz,² Kenneth C. Hayes,² Kaijun Lu ³¹Department of Physical and Environmental Sciences, Texas A&M University, Corpus Christi, Texas; ²Department of Life Sciences, Texas A&M University, Corpus Christi, Texas; ³Marine Science Institute, University of Texas at Austin, Port Aransas, Texas**Scientific Significance Statement**

Photochemical remineralization of dissolved organic carbon (DOC) is considered an important DOC sink in the aquatic environments, and previous studies revealed that photochemical reactions enrich the heavy carbon isotope (^{13}C) in the residual DOC pool. To date, few studies have examined the significance of photomineralization in subtropical estuaries, particularly those subject to eutrophication and high DOC levels. We found that photomineralization plays an important role in not only removing DOC, but also shifting the stable isotopic composition of residual DOC to be more ^{13}C -depleted, contrary to findings in other coastal and open ocean environments.

Abstract

The effect of photomineralization on the carbon cycle in a eutrophic, semiarid estuary (Baffin Bay, Texas) was investigated using closed-system incubations. Photochemical production rate of dissolved inorganic carbon ranged from 0.16 to 0.68 $\mu\text{M hr}^{-1}$, with a daily removal of 0.3~1.5% of the standing stock of dissolved organic carbon (DOC). The photomineralization rate was negatively correlated with chlorophyll *a* concentration, suggesting that plankton-derived DOC was less photoreactive to solar radiation. The stable carbon isotope composition ($\delta^{13}\text{C} \sim -18.6\text{‰}$) of degraded DOC, as calculated using the DIC “Keeling” plot, further indicated high photochemical lability of ^{13}C -enriched DOC in this semiarid environment. Our finding showed that photomineralization of ^{13}C -enriched DOC is an important component of carbon cycle in this system, and this process does not necessarily remove ^{13}C -depleted organic carbon as observed in other coastal systems.

*Correspondence: hwangde@udel.edu

Associate editor: Alberto Borges

Present address: School of Marine Science and Policy, University of Delaware, Newark, DE, United States

Author Contribution Statement: HW and XH came up with the research question. HW designed the experiment and wrote the manuscript with helpful input from XH and MW. KH conducted field surveys and provided DOC and Chl data. KL carried out an additional experiment to examine the possible effect of Hg on the oxidation of organic carbon.

Data Availability Statement: Data are available at <https://doi.org/10.25921/n1zz-qg34>.

Additional Supporting Information may be found in the online version of this article.

This is an open access article under the terms of the Creative Commons Attribution License, which permits use, distribution and reproduction in any medium, provided the original work is properly cited.

Past studies showed that photomineralization of dissolved organic carbon (DOC) in the aquatic environment is a major removal mechanism for terrestrially derived DOC (Miller and Zepp 1995; Hernes and Benner 2003; Aarnos et al. 2018). For example, at least 15% of Rio Negro (a tributary of the Amazon River) DOC is photoreactive after sunlight exposure for 27 h, and the photomineralization rate of DOC ($\sim 4.0 \mu\text{M hr}^{-1}$) is approximately sevenfold greater than that of bacterial DOC utilization in Rio Negro surface waters (Amon and Benner 1996). Similarly, Congo River DOC is also shown to be highly photoactive, with over 95% decrease in lignin phenol concentration after a ~ 38 -day natural sunlight exposure equivalence (Spencer et al. 2009). Overall, photomineralization of DOC accounts for 70–90% of total DOC processed in the water column of Arctic lakes and rivers (Cory et al. 2014). Photomineralization that converts DOC into dissolved inorganic carbon (DIC) is also an important sink for organic carbon (OC) in both coastal and open ocean environments (Vodacek et al. 1997; Tracy and Sybil 2001; Brinkmann et al. 2003; Nieto-Cid et al. 2006; Stubbins et al. 2006; Wang et al. 2009; Xie et al. 2009; White et al. 2010; Stubbins et al. 2011; Reader and Miller 2012; Fichot and Benner 2014). In addition to photodegradation induced direct mineralization, Fichot and Benner (2014) reported that photomineralization can significantly enhance biomineralization ($\sim 50\%$) in the mixed layer in a large river-influenced ocean margin in the northern Gulf of Mexico.

Past studies have shown that DOC of different origins may have different photoreactivities. For example, Opsahl and Benner (1998) reported rapid photochemical degradation of terrestrially derived lignin phenols in seawater. This finding was supported by the changes in DOC stable carbon isotopic composition before and after photochemical alterations of soil solutions, river water, and estuarine water. Furthermore, ^{13}C -depleted DOC is selectively removed due to preferential photomineralization of lignin-derived and aromatic-rich compounds, as demonstrated by strong correlation between the loss of lignin phenol and increase in $\delta^{13}\text{C}_{\text{DOC}}$ during irradiation (Spencer et al. 2009). Thus, photochemical reactions generally increase $\delta^{13}\text{C}_{\text{DOC}}$ (2–3‰) in the residual DOC pool (Opsahl and Zepp 2001; Spencer et al. 2009; Lu et al. 2013), and this increase was reported to be up to 6‰ after a 459-day exposure to surface solar irradiation (Vähätalo and Wetzel 2008).

Baffin Bay is located on the semiarid south Texas coast in the northwestern Gulf of Mexico. Since 1989, Baffin Bay and adjacent Upper Laguna Madre have experienced large, prolonged blooms of the “brown tide” phytoplankton species, *Aureoumbra lagunensis* (Wetz et al. 2017). A previous study showed that Baffin Bay has exceptionally high DOC concentrations compared to other estuaries on the Texas coast and elsewhere (Wetz et al. 2017). However, the reason for this high DOC concentration is not entirely clear. It is likely that ephemeral loadings from the watershed, in-situ biological

production, and evaporation-induced concentrating effect all play some role (Wetz et al. 2017; Montagna et al. 2018).

There are a few OC sources in Baffin Bay including phytoplankton, seagrasses, terrestrial OC, algal mats, epiphytes, and benthic algae. Among them, $\delta^{13}\text{C}$ of in situ produced OC (phytoplankton), including the brown tide (*Aureoumbra lagunensis*) bloom, is $\sim -20.3\text{‰}$ (Buskey et al. 1999). Seagrass in lower Baffin Bay with an average $\delta^{13}\text{C}$ of $\sim -10\text{‰}$ (Lebreton et al. 2016). $\delta^{13}\text{C}_{\text{POC}}$ in streams draining into Baffin Bay was generally $\sim -23\text{‰}$ (Wang et al. 2018). Despite the potentially different OC sources, the more negative $\delta^{13}\text{C}_{\text{POC}}$ (-25.8‰ to -29.0‰) observed after a period of prolonged drought (November 2014 to March 2015) remains to be explained (Wang et al. 2018).

Given that Baffin Bay is subjected to strong solar irradiation and warm water temperature most of the year, our experiment was designed to address two main hypotheses: (1) photomineralization could be an important OC sink; (2) photomineralization could change $\delta^{13}\text{C}$ of the residual DOC overtime. To test these hypotheses, we quantified DIC production rates and measured $\delta^{13}\text{C}$ of DIC overtime using a series of closed-system incubations under natural sunlight. The cumulative number of estuaries in semiarid/arid regions is close to that of classic river-dominated estuaries. As a result, these semiarid/arid estuaries can have a significant areal footprint (Largier 2010; Potter et al. 2010). Therefore, findings presented here highlight a critically important process in the estuarine OC cycle.

Method

Near-surface (<0.5 m) water samples were collected from two stations along the main channel of Baffin Bay (BB3 and BB6 in Fig. 1) on 11 August 2017. Both near-surface and near-bottom (<0.5 m above the sediment) water samples were collected at these two stations on 18 September 2017. For the

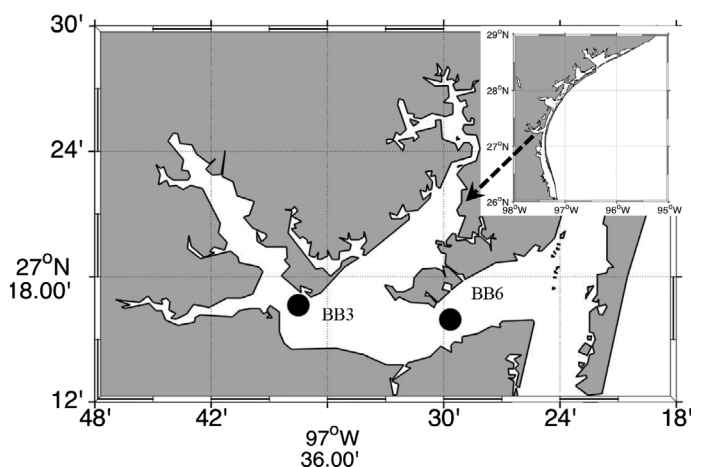


Fig. 1. Sampling stations in Baffin Bay. Note the inserted panel shows the relative location of Baffin Bay in the northwestern Gulf of Mexico.

August 2017 experiment, both filtered (through precombusted Whatman GF/F filters, pore size = 0.7 μm) and whole water samples were distributed into ground-neck 1000-mL quartz bottles. Only filtered water was used in the September 2017 experiment. There was no duplicate bottle for all incubations.

DOC and chlorophyll *a* samples were collected at the beginning of the incubation. DOC concentration was determined using a Shimadzu TOC-V with self-contained magnetic stirrers. Laboratory check standards were used in conjunction with Certified Reference Material Program deep seawater standards of known DOC concentration ($43.5 \pm 2.2 \mu\text{mol L}^{-1}$). For chlorophyll *a* analysis, a known volume of water sample was gently filtered through Whatman GF/F filters (pore size = 0.7 μm), which were then stored frozen at -20°C until analysis. Chlorophyll *a* was extracted from the filters by soaking them for 18–24 h in 90% HPLC-grade acetone at -20°C , after which the concentration was determined fluorometrically with a Turner Trilogy fluorometer without acidification, using an excitation wavelength of 430 nm and an emission wavelength of 663 nm.

Microbial activity in all incubating bottles was stopped by adding 400 μL saturated HgCl_2 solution, and the bottles were then closed and exposed to natural sunlight outdoors. The bottle stoppers were secured with Parafilm[®] and placed in a plastic tray (89.9 cm \times 42.5 cm \times 14.9 cm) filled with tap water. The water level in the tray was maintained near the bottle neck, which was about 14.5 cm in height. Water temperature was not controlled and varied with air temperature. Aliquots of water samples ($\sim 12 \text{ mL}$) were extracted every 4–5 d using syringes from the 1000 mL quartz bottles for DIC analyses (both concentration and stable carbon isotope, or $\delta^{13}\text{C}_{\text{DIC}}$). Care was taken to minimize the opening time (60–90 s) of bottle stoppers during sample extraction. $\delta^{13}\text{C}_{\text{DIC}}$ samples were saved in 2 mL borosilicate autosampler vials (Restek[®]) with natural rubber septa lined open-top aluminum caps. DIC samples were stored in 4 mL borosilicate vials, which were tightly closed using phenolic screw caps with PTFE-faced rubber liner. $\delta^{13}\text{C}_{\text{DIC}}$ and DIC analyses were finished in 2 weeks after the experiment. The $\delta^{13}\text{C}_{\text{DOC}}$ samples were collected at the beginning and the end of each filtered water incubation and preserved in 40 mL Fisher brand borosilicate glass EPA vials with Teflon-lined silicone septa.

The analytical methods for DIC, $\delta^{13}\text{C}_{\text{DIC}}$, and $\delta^{13}\text{C}_{\text{DOC}}$ were the same as those used in Wang et al. (2018). Briefly, DIC was measured with an infrared CO_2 detector-based DIC analyzer (AS-C3, Apollo SciTech Inc.). Certified Reference Materials from A. G. Dickson, Scripps Institution of Oceanography were used as an independent data quality control. The precisions for DIC was within $\pm 2 \mu\text{mol L}^{-1}$ ($\pm 0.1\%$, Chen et al. 2015). $\delta^{13}\text{C}_{\text{DIC}}$ samples were analyzed in J. Brandes' lab at Skidaway Institute of Oceanography, University of Georgia. They were determined on a Thermo Fisher Delta V isotope ratio mass spectrometer (IRMS) with a GasBench II preparation module for trace gas samples. The analytical precision was $\pm 0.1\%$ (Brandes 2009). $\delta^{13}\text{C}_{\text{DOC}}$ samples were preserved at $\text{pH} \sim 2$ by

adding one drop of concentrated HCl. The $\delta^{13}\text{C}_{\text{DOC}}$ samples were analyzed by C. Osburn's lab at North Carolina State University. They were measured with a combination of an Aurora 1030C high-temperature catalytic conversion DOC analyzer, a molecular sieve trap, and a continuous-flow IRMS. The precision of the $\delta^{13}\text{C}_{\text{DOC}}$ analysis was $\pm 0.2\%$ (Lalonde et al. 2014a).

Because the gaseous photoproducts of DOC are dominated by DIC (CO_2 production was about 15 to 22 times larger than carbon monoxide production) (Miller and Moran 1997; Powers and Miller 2015), we only measured DIC concentration in this study. Only daylight hours were considered in the photomineralization rate calculations.

Results and discussion

Organic carbon photomineralization rates

In the August experiment, exposure to sunlight resulted in an increase in DIC in both whole and filtered waters (Figs. 2A,B, Table S1). The whole water incubations only resulted in slightly higher DIC accumulation compared to the filtered water at both Station BB3 (222 vs. 191 μM) and BB6 (275 vs. 254 μM), indicating that the majority of photoreactive OC was in the DOC pool (Fig. 2). This result was consistent with a previous study in which the contribution of particulate organic carbon (POC) accounts for 11% DIC photoproduction in the lower St. Lawrence Estuary (Xie and Zafriou 2009). Note, this experiment was temporarily interrupted between 23 August and 31 August 2017 as the incubating bottles had to be moved indoors prior to Hurricane Harvey. Neither DIC nor $\delta^{13}\text{C}_{\text{DIC}}$ changed during this lightless period (Figs. 2A,B), indicative of gas-tightness of our incubation bottles and effectiveness of adding HgCl_2 in arresting biological activities. The average daily irradiation time was 13.0 h from 11 August to 16 September based on the solar radiation data collected from 1977 to 1994 at Corpus Christi International Airport (CCIA, http://redc.nrel.gov/solar/old_data/nsrdb/1991-2005/tmy3/). Therefore, the DIC production rate (total DIC accumulation/ $[28 \text{ d} \times 13 \text{ h d}^{-1}]$) for the filtered and whole water was $0.52 \sim 0.70 \mu\text{M hr}^{-1}$, and $0.61 \sim 0.76 \mu\text{M hr}^{-1}$, respectively. These rates were close to the photomineralization rate ($0.84 \mu\text{M hr}^{-1}$) based on 38 d's natural light incubation in Congo River, and the average photochemical DIC production rate ($0.75 \mu\text{M hr}^{-1}$) measured from Sapelo Island marsh, Mississippi River plume and Suwanee River within $< 200 \text{ h}$ of irradiation (Miller and Zepp 1995).

In addition to oxidizing DOC to DIC and carbon monoxide (CO), solar irradiation can also alter spectral and molecular properties of DOC by transforming it into biologically degradable lower molecular weight carboxylic acids (oxalic, malonic, formic, and acetic acid). For example, the photochemically produced carboxylic acid carbon contributes up to 34% of DIC production (Bertilsson and Tranvik 2000; Brinkmann et al. 2003). Assuming the ratio between photoproduced carboxylic acids and DIC, and that between CO and DIC in Baffin Bay

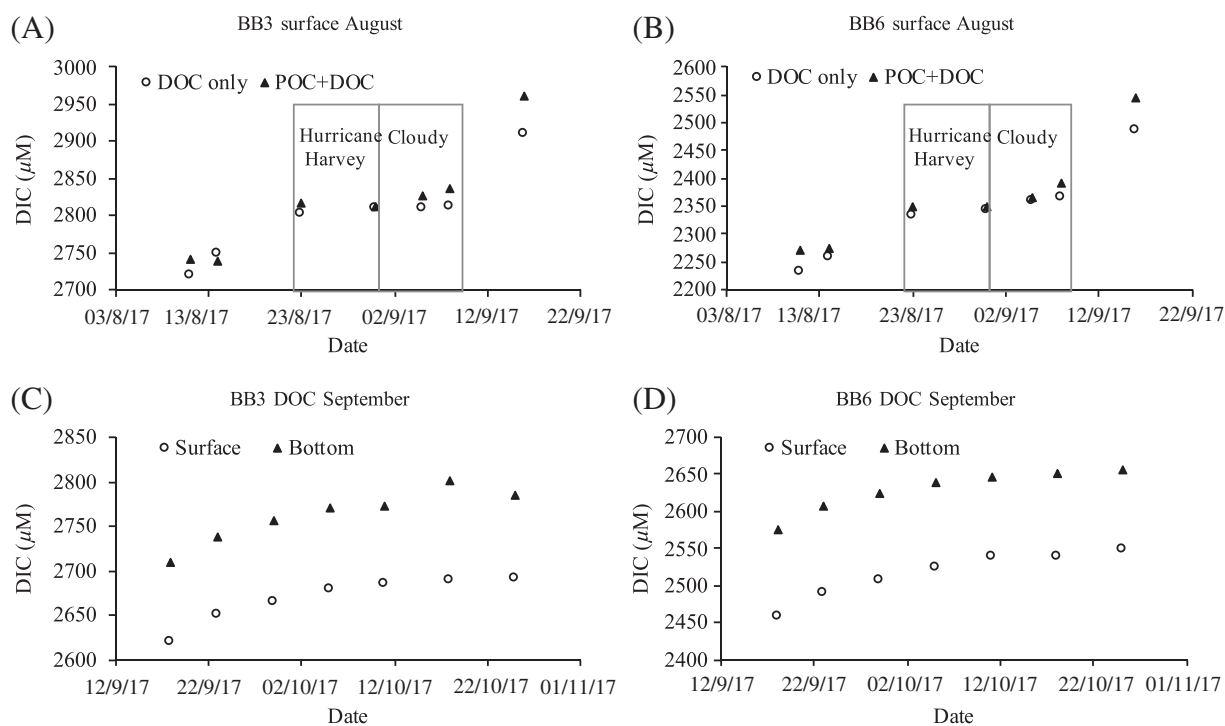


Fig. 2. DIC concentration changes in the filtered (DOC only) and whole water (DOC+POC) from BB3 and BB6 surface during the 11 August–16 September experiment (A, B); and DIC concentration changes in filtered surface and bottom waters from BB3 and BB6 during the 18 September–25 October experiment (C, D).

was the same as previous studies in other systems, the total photomineralized DOC should be 1.4 times of DIC increasing rate. Then, the percentage of initial DOC that was photoactive based on the August experiment ranged from 29.2% to 54.9%. This then suggests that about one third to a half of DOC pool was photochemically reactive. The net productivity in surface water of Station BB6 and Station BB3 was $2.7 \mu\text{M C hr}^{-1}$ in August 2017 (Wetz, unpublished data). Therefore, photomineralization of OC to DIC could remove as much as 40% of the net productivity in surface water based on the August 2017 experiment.

DIC concentrations also increased in the filtered waters from both surface and bottom during the incubation from 18 September to 25 October 2017, although the values appeared to level off over time (Figs. 2C,D). In addition, DIC accumulation in this incubation was much lower than in August, ranging from 71 to $91 \mu\text{M}$ (vs. $191\text{--}254 \mu\text{M}$ DIC increase during similar incubation span, Table S1). Photomineralization rates were almost the same for both surface and bottom waters (Figs. 2C,D). The average daily irradiation time was 12.1 h from 18 September to 25 October (CCIA data). Therefore, the photomineralization rate (total DIC accumulation/[$37 \text{ d} \times 12.1 \text{ h d}^{-1}$]) ranged from 0.16 to $0.20 \mu\text{M hr}^{-1}$, which was about 29% of the rate measured in August. Nevertheless, these lower DIC photoproduction rates in the September experiment was still higher than the

maximum rate ($0.04 \mu\text{M hr}^{-1}$) in the southeastern Beaufort Sea (solar radiation $<4 \text{ h}$, Xie et al. 2009), and close to the rate (0.2 to $0.3 \mu\text{M hr}^{-1}$) in Delaware Estuary (solar radiation $<8 \text{ h}$, White et al. 2010). If we take the initial 5 d only, daily DIC production rates were $0.47\text{--}0.55 \mu\text{M hr}^{-1}$, closer to the rates observed in the August incubations. Similar to previous studies (Vodacek et al. 1997; Porcal et al. 2013; Vachon et al. 2016), our findings highlight the potential importance of seasonal variability in photomineralization rates in Baffin Bay, which merit further study.

We did not directly measure the solar irradiance during the experiment, so we used the average daily solar irradiance from NCEP/NCAR Reanalysis 1 in area between Baffin Bay and Corpus Christi (27.6186°N , 262.5°E , https://www.esrl.noaa.gov/psd/data/gridded/data.ncep.reanalysis.other_flux.html) to represent the average solar irradiance. The daily average Downward Solar Radiation Flux during these two experiments were 292 W m^{-2} and 223 W m^{-2} , respectively. With the daily light time hours (13 h vs 12.1 h), the daily average solar irradiance was 3.8 kWh m^{-2} and 2.7 kWh m^{-2} during our August and September experiments, respectively. Therefore, the solar irradiance-normalized photoproduction DIC rates were estimated to be $0.14\text{--}0.20$ and $0.06\text{--}0.08 \mu\text{M hr}^{-1} \text{ kWh}^{-1} \text{ m}^2$ during these two periods, respectively. During these two experiments, average ambient temperature was $27.1 \pm 2.4^\circ\text{C}$ and $25.4 \pm 3.5^\circ\text{C}$, respectively. This small temperature

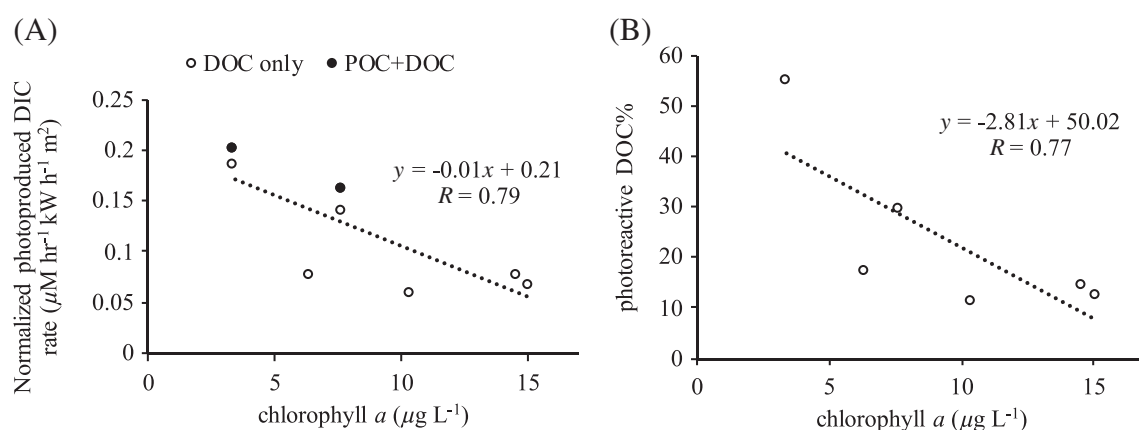


Fig. 3. (A) The relationship between normalized photochemical DIC production rate and chlorophyll *a* concentration. (B) The relationship between photoactive DOC% and chlorophyll *a* concentration.

difference (less than 2°C) should only have limited effect on the DIC photoproduction rate because of the weak temperature dependence (Zhang et al. 2006) of CO quantum yield (CO is used as a proxy for CO_2 photoproduction). As temperature is likely of minor importance in the photomineralization rates in the two experiments, the rates difference could be caused by the difference in the DOC characteristics (i.e., photochemical lability). In fact, the photoreactive DOC% ranged only from 11.1% to 16.7% based on September experiment, which was much lower than that in August (29.2% to 54.9%).

Both normalized DIC production rate and photoactive DOC % was negatively correlated with chlorophyll *a* concentration (Fig. 3). This negative correlation suggests that DOC in Baffin Bay was less photoreactive under high phytoplankton biomass condition (as shown in the September experiment, Table S1). This interpretation is consistent with previous studies that the terrestrial DOC is susceptible to faster photomineralization rate, while the plankton-derived DOC is more resistant to solar radiation (Thomas and Lara 1995; Bertilsson and Tranvik 2000; Obernosterer and Benner 2004). We should note that the negative relationship in Fig. 3 was limited by the small number of observations ($n = 8$) and relatively narrow chlorophyll *a* range ($3.4\sim 15.1 \mu\text{g L}^{-1}$, Table S2), thus more work is clearly needed to further examine photomineralization rate at higher chlorophyll *a* condition ($>15 \mu\text{g L}^{-1}$) during algal bloom events, such as the “brown tide”. Nonetheless, the results are consistent with previous work showing the importance of DOC quality to photomineralization rate (Opsahl and Benner 1998; Obernosterer and Benner 2004). Meanwhile, as the water residence time in Baffin Bay is over 1 yr and there was no significant precipitation between the two sampling events (Hurricane Harvey did not affect this area significantly), the water sample collected for the September experiment had been exposed to solar radiation for an additional month. It is thus reasonable to speculate that part of the photoactive fraction may have been decomposed in September, which might have led to lower observed

photomineralization rate in the September experiment. However, this explanation would need further verification.

$\delta^{13}\text{C}$ of CO_2 produced in photochemical reaction

Using the “Keeling” plot, the $\delta^{13}\text{C}$ of photoproduced DIC during the August incubation was calculated as -9.1‰ and -18.6‰ in BB6 and BB3 surface waters, respectively (Fig. 4A,B, Table S2). The regressions between the whole and filtered waters were not significantly different (analysis of covariance, p value was 0.87 and 0.69 for BB3 and BB6, respectively). The $\delta^{13}\text{C}$ of photoproduced DIC in the September experiment (Fig. 4C,D) ranged from -17.9‰ to -19.3‰ . Note, BB6 bottom water had the intercept of -23.5‰ if excluding the last three data points (Fig. 4D). It is possible that gas leakage occurred for this single incubation thus the result was not included in the discussion, despite that the earlier incubations showed the overall gas-tightness of these incubation bottles.

The initial $\delta^{13}\text{C}_{\text{DOC}}$ of this study was $-19.9 \pm 0.7\text{‰}$ in surface Station BB3 and BB6 from August to September experiments, then it decreased significantly after the incubation (Fig. 5, paired t -test, $p = 0.05$), as a result of preferential removal of heavy carbon during the sunlight exposure, if excluding the BB3 bottom water in the September incubation in which the ending $\delta^{13}\text{C}_{\text{DOC}}$ was heavier than the initial value (Fig. 5, Table S2). Using DOC concentrations during each incubation and stable isotopic mass balance, we calculated the $\delta^{13}\text{C}$ of photomineralized DOC, which averaged $-18.1 \pm 0.8\text{‰}$. This value was statistically indistinguishable to the value calculated using the Keeling method above ($p = 0.8$). Preferential photomineralization of isotopically heavy OC ($\sim -18.6\text{‰}$), in contrast to previous studies that found isotopically lighter OC is more photochemical labile (Opsahl and Zepp 2001; Vähätalo and Wetzel 2008; Lalonde et al. 2014b), may result from the abundant C4 plants in Baffin Bay’s watershed.

A previous study showed that $\delta^{13}\text{C}_{\text{DOC}}$ and $\delta^{13}\text{C}_{\text{POC}}$ values are very similar in coastal or estuarine environment

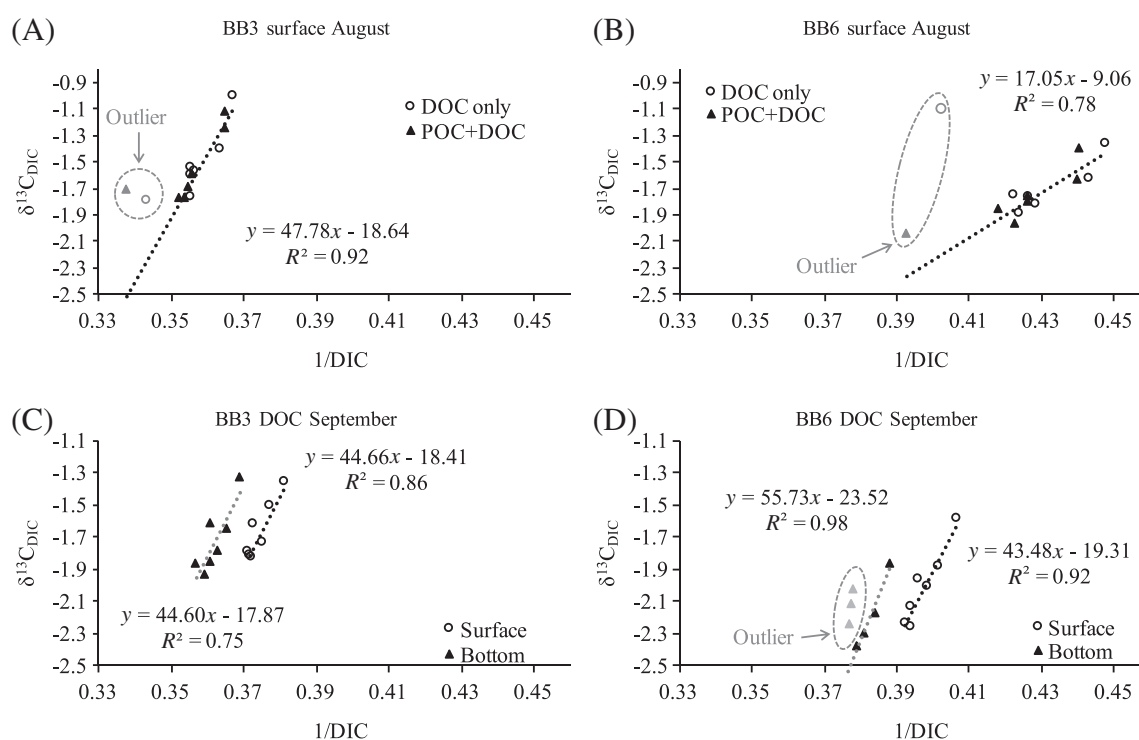


Fig. 4. The $\delta^{13}\text{C}_{\text{DIC}}$ change in filtered or whole water in the 11 August–16 September experiment (A, B), and in filtered surface or bottom water in the 18 September 18–25 October experiment (C, D). Note, the outliers in panels A, B, and D were defined as greater than five times of the mean Cook's distance (Neter et al. 1996).

(Raymond and Bauer 2001). Similarly, the $\delta^{13}\text{C}$ of bulk DOC ($-22.6 \pm 2.6\text{‰}$) in Baffin Bay was close to $\delta^{13}\text{C}_{\text{POC}}$ after a flooding event (Wang et al. 2018). If we took the average DOC concentration in Baffin Bay ($850 \pm 105 \mu\text{M}$, Wetz et al. 2017) and $\delta^{13}\text{C}_{\text{DOC}}$ ($-22.6 \pm 2.6\text{‰}$, Wang et al. 2018) as the starting conditions, and assume half of the total DOC was photoreactive (Table S2), then the residual OC pool would decrease from -22.6‰ to -26.6‰ by preferential photomineralization of OC that has $\delta^{13}\text{C} = -18.6\text{‰}$. The calculated $\delta^{13}\text{C}$ of residual OC will be more negative if the photoactive DOC% was higher, and was closer to the measured $\delta^{13}\text{C}_{\text{POC}}$

($-28.1 \pm 0.6\text{‰}$, November 2014–March 2015, Wang et al. 2018) after an extended drought. Therefore, photomineralization could be the reason for the mismatch between the more negative bulk $\delta^{13}\text{C}_{\text{OC}}$ and much isotopically heavier OC sources delivered to this water body. This interpretation then would imply the importance of photomineralization on the carbon cycle in this system, which has sluggish water exchange with the coastal ocean.

Implications and conclusions

Based on our estimates of DOC photomineralization rates, it appeared that the photochemical reaction was an important sink for DOC in Baffin Bay, and the daily removal rate was $\sim 0.3\%$ to 1.5% of bulk DOC in surface water. In contrast to previous studies that revealed lighter carbon being preferentially converted, we found that the photoreactive OC was more $\delta^{13}\text{C}$ -enriched compared to the bulk carbon (POC and DOC) pool in Baffin Bay. Further investigation on stream/river $\delta^{13}\text{C}_{\text{OC}}$ and compound-specific $\delta^{13}\text{C}$ will be helpful to better define the carbon sources for photochemical reactions in this system. Our incubations based on only two experiments also showed that the photomineralization had strong seasonal variations, due mostly to DOC photoreactivity. DOC was less photoreactive under high chlorophyll *a* condition ($\sim 15 \mu\text{g L}^{-1}$) in Baffin Bay. One of the major features of Baffin Bay is prolonged

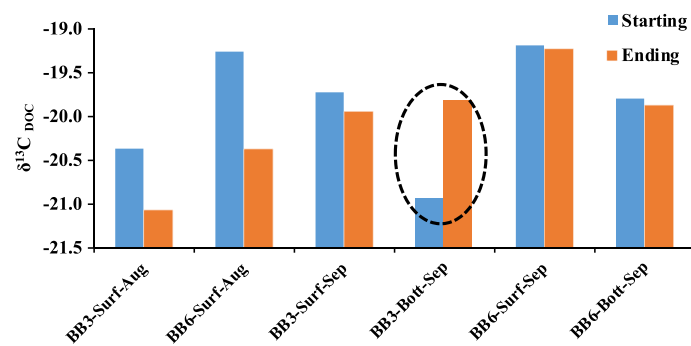


Fig. 5. $\delta^{13}\text{C}_{\text{DOC}}$ before and after water incubation. The result of BB3-bottom-september (circled) were different from others for reasons that are unclear (see text for details).

(months-years) “brown tide”. However, our incubations did not overlap with a brown tide bloom event. Future studies should examine both photochemical and biological lability of brown tide biomass, which can be a significant organic carbon pool and should exert strong control on carbon cycle in this system.

References

- Aarnos, H., Y. Gélinas, V. Kasurinen, Y. Gu, V.-M. Puupponen, and A. V. Vähätalo. 2018. Photochemical mineralization of terrigenous DOC to dissolved inorganic carbon in ocean. *Global Biogeochem. Cycles* **32**: 250–266. doi:10.1002/2017GB005698
- Amon, R. M. W., and R. Benner. 1996. Photochemical and microbial consumption of dissolved organic carbon and dissolved oxygen in the Amazon River system. *Geochim. Cosmochim. Acta* **60**: 1783–1792. doi:10.1016/0016-7037(96)00055-5
- Bertilsson, S., and L. J. Tranvik. 2000. Photochemical transformation of dissolved organic matter in lakes. *Limnol. Oceanogr.* **45**: 753–762. doi:10.4319/lo.2000.45.4.0753
- Brandes, J. A. 2009. Rapid and precise $\delta^{13}\text{C}$ measurement of dissolved inorganic carbon in natural waters using liquid chromatography coupled to an isotope-ratio mass spectrometer. *Limnol. Oceanogr. Methods* **7**: 730–739. doi:10.4319/lom.2009.7.730
- Brinkmann, T., P. Hörsch, D. Sartorius, and F. H. Frimmel. 2003. Photoformation of low-molecular-weight organic acids from brown water dissolved organic matter. *Environ. Sci. Technol.* **37**: 4190–4198. doi:10.1021/es0263339
- Buskey, E., K. Dunton, and P. Parker. 1999. Variations in stable carbon isotope ratio of the copepod *Acartia tonsa* during the onset of the Texas brown tide. *Estuaries* **22**: 995–1003. doi:10.2307/1353078
- Chen, B., W.-J. Cai, and L. Chen. 2015. The marine carbonate system of the Arctic Ocean: Assessment of internal consistency and sampling considerations, summer 2010. *Mar. Chem.* **176**: 174–188. doi:10.1016/j.marchem.2015.09.007
- Cory, R. M., C. P. Ward, B. C. Crump, and G. W. Kling. 2014. Sunlight controls water column processing of carbon in arctic fresh waters. *Science* **345**: 925–928. doi:10.1126/science.1253119
- Fichot, C. G., and R. Benner. 2014. The fate of terrigenous dissolved organic carbon in a river-influenced ocean margin. *Global Biogeochem. Cycles* **28**: 300–318. doi:10.1002/2013GB004670
- Hernes, P. J., and R. Benner. 2003. Photochemical and microbial degradation of dissolved lignin phenols: Implications for the fate of terrigenous dissolved organic matter in marine environments. *J. Geophys. Res. Oceans* **108**: 3291. doi:10.1029/2002JC001421
- Lalonde, K., P. Middlestead, and Y. Gélinas. 2014a. Automation of $^{13}\text{C}/^{12}\text{C}$ ratio measurement for freshwater and seawater DOC using high temperature combustion. *Limnol. Oceanogr. Methods* **12**: 816–829. doi:10.4319/lom.2014.12.816
- Lalonde, K., A. V. Vähätalo, and Y. Gélinas. 2014b. Revisiting the disappearance of terrestrial dissolved organic matter in the ocean: A $\delta^{13}\text{C}$ study. *Biogeosciences* **11**: 3707–3719. doi:10.5194/bgd-10-17117-2013
- Largier, J. 2010. Low-inflow estuaries: Hypersaline, inverse, and thermal scenarios, p. 247–272. In A. Valle-Levinson [ed.], *Contemporary issues in estuarine physics*. Cambridge Univ. Press.
- Lebreton, B., and others. 2016. Origin, composition and quality of suspended particulate organic matter in relation to freshwater inflow in a South Texas estuary. *Estuar. Coast. Shelf Sci.* **170**: 70–82. doi:10.1016/j.ecss.2015.12.024
- Lu, Y., J. E. Bauer, E. A. Canuel, Y. Yamashita, R. M. Chambers, and R. Jaffé. 2013. Photochemical and microbial alteration of dissolved organic matter in temperate headwater streams associated with different land use. *J. Geophys. Res. Biogeo.* **118**: 566–580. doi:10.1002/jgrg.20048
- Miller, W. L., and M. A. Moran. 1997. Interaction of photochemical and microbial processes in the degradation of refractory dissolved organic matter from a coastal marine environment. *Limnol. Oceanogr.* **42**: 1317–1324. doi:10.4319/lo.1997.42.6.1317
- Miller, W. L., and R. G. Zepp. 1995. Photochemical production of dissolved inorganic carbon from terrestrial organic matter: Significance to the oceanic organic carbon cycle. *Geophys. Res. Lett.* **22**: 417–420. doi:10.1029/94GL03344
- Montagna, P. A., X. Hu, T. A. Palmer, and M. Wetz. 2018. Effect of hydrological variability on the biogeochemistry of estuaries across a regional climatic gradient. *Limnol. Oceanogr.* **63**: 2465–2478. doi:10.1002/lno.10953
- Neter, J., M. H. Kutner, C. J. Nachtsheim, and W. Wasserman. 1996. *Applied linear statistical models*. Chicago: Irwin.
- Nieto-Cid, M., X. A. Álvarez-Salgado, and F. F. Pérez. 2006. Microbial and photochemical reactivity of fluorescent dissolved organic matter in a coastal upwelling system. *Limnol. Oceanogr.* **51**: 1391–1400. doi:10.4319/lo.2006.51.3.1391
- Obernosterer, I., and R. Benner. 2004. Competition between biological and photochemical processes in the mineralization of dissolved organic carbon. *Limnol. Oceanogr.* **49**: 117–124. doi:10.4319/lo.2004.49.1.0117
- Opsahl, S., and R. Benner. 1998. Photochemical reactivity of dissolved lignin in river and ocean waters. *Limnol. Oceanogr.* **43**: 1297–1304. doi:10.4319/lo.1998.43.6.1297
- Opsahl, S. P., and R. G. Zepp. 2001. Photochemically-induced alteration of stable carbon isotope ratios ($\delta^{13}\text{C}$) in terrigenous dissolved organic carbon. *Geophys. Res. Lett.* **28**: 2417–2420. doi:10.1029/2000GL012686
- Porcal, P., P. J. Dillon, and L. A. J. B. Molot. 2013. Seasonal changes in photochemical properties of dissolved organic

- matter in small boreal streams. *Biogeosciences* **10**: 5533–5543. doi:[10.5194/bg-10-5533-2013](https://doi.org/10.5194/bg-10-5533-2013)
- Potter, P., N. Ramankutty, E. M. Bennett, and S. D. Donner. 2010. Characterizing the spatial patterns of global fertilizer application and manure production. *Earth Interact.* **14**: 1–22. doi:[10.1175/2009EI288.1](https://doi.org/10.1175/2009EI288.1)
- Powers, L. C., and W. L. Miller. 2015. Photochemical production of CO and CO₂ in the northern Gulf of Mexico: Estimates and challenges for quantifying the impact of photochemistry on carbon cycles. *Mar. Chem.* **171**: 21–35. doi:[10.1016/j.marchem.2015.02.004](https://doi.org/10.1016/j.marchem.2015.02.004)
- Raymond, P. A., and J. E. Bauer. 2001. Use of ¹⁴C and ¹³C natural abundances for evaluating riverine, estuarine, and coastal DOC and POC sources and cycling: A review and synthesis. *Org. Geochem.* **32**: 469–485. doi:[10.1016/S0146-6380\(00\)00190-X](https://doi.org/10.1016/S0146-6380(00)00190-X)
- Reader, H., and W. Miller. 2012. Variability of carbon monoxide and carbon dioxide apparent quantum yield spectra in three coastal estuaries of the South Atlantic Bight. *Biogeosciences* **9**: 4279. doi:[10.5194/bg-9-4279-2012](https://doi.org/10.5194/bg-9-4279-2012)
- Spencer, R. G. M., and others. 2009. Photochemical degradation of dissolved organic matter and dissolved lignin phenols from The Congo River. *J. Geophys. Res. Biogeo.* **114**: G03010. doi:[10.1029/2009JG000968](https://doi.org/10.1029/2009JG000968)
- Stubbins, A., G. Uher, C. S. Law, K. Mopper, C. Robinson, and R. C. Upstill-Goddard. 2006. Open-ocean carbon monoxide photoproduction. *Deep-Sea Res. II Top. Stud. Oceanogr.* **53**: 1695–1705. doi:[10.1016/j.dsr2.2006.05.011](https://doi.org/10.1016/j.dsr2.2006.05.011)
- Stubbins, A., C. Law, G. Uher, and R. Upstill-Goddard. 2011. Carbon monoxide apparent quantum yields and photoproduction in the Tyne estuary. *Biogeosciences* **8**: 703–713. doi:[10.5194/bg-8-703-2011](https://doi.org/10.5194/bg-8-703-2011)
- Thomas, D. N., and R. J. Lara. 1995. Photodegradation of algal derived dissolved organic carbon. *Mar. Ecol. Prog. Ser.* **116**: 309–310. doi:[10.3354/meps116309](https://doi.org/10.3354/meps116309)
- Tracy, N. W., and P. S. Sybil. 2001. Photochemical and microbial degradation of external dissolved organic matter inputs to rivers. *Aquat. Microb. Ecol.* **24**: 27–40. doi:[10.3354/ame024027](https://doi.org/10.3354/ame024027)
- Vachon, D., J.-F. Lapierre, and P. A. del Giorgio. 2016. Seasonality of photochemical dissolved organic carbon mineralization and its relative contribution to pelagic CO₂ production in northern lakes. *J. Geophys. Res. Biogeo.* **121**: 864–878. doi:[10.1002/2015JG003244](https://doi.org/10.1002/2015JG003244)
- Vähätalo, A. V., and R. G. Wetzel. 2008. Long-term photochemical and microbial decomposition of wetland-derived dissolved organic matter with alteration of 13C:12C mass ratio. *Limnol. Oceanogr.* **53**: 1387–1392. doi:[10.4319/lo.2008.53.4.1387](https://doi.org/10.4319/lo.2008.53.4.1387)
- Vodacek, A., N. V. Blough, M. D. DeGrandpre, and R. K. Nelson. 1997. Seasonal variation of CDOM and DOC in the Middle Atlantic Bight: Terrestrial inputs and photooxidation. *Limnol. Oceanogr.* **42**: 674–686. doi:[10.4319/lo.1997.42.4.0674](https://doi.org/10.4319/lo.1997.42.4.0674)
- Wang, W., C. G. Johnson, K. Takeda, and O. C. Zafriou. 2009. Measuring the photochemical production of carbon dioxide from marine dissolved organic matter by pool isotope exchange. *Environ. Sci. Technol.* **43**: 8604–8609. doi:[10.1021/es901543e](https://doi.org/10.1021/es901543e)
- Wang, H., X. Hu, M. Wetz, and K. Hayes. 2018. Oxygen consumption and organic matter remineralization in two subtropical, eutrophic coastal embayments. *Environ. Sci. Technol.* **52**: 13004–13014. doi:[10.1021/acs.est.8b02971](https://doi.org/10.1021/acs.est.8b02971)
- Wetz, M. S., E. K. Cira, B. Sterba-Boatwright, P. A. Montagna, T. A. Palmer, and K. C. Hayes. 2017. Exceptionally high organic nitrogen concentrations in a semi-arid South Texas estuary susceptible to brown tide blooms. *Estuar. Coast. Shelf Sci.* **188**: 27–37. doi:[10.1016/j.ecss.2017.02.001](https://doi.org/10.1016/j.ecss.2017.02.001)
- White, E. M., D. J. Kieber, J. Sherrard, W. L. Miller, and K. Mopper. 2010. Carbon dioxide and carbon monoxide photoproduction quantum yields in the Delaware estuary. *Mar. Chem.* **118**: 11–21. doi:[10.1016/j.marchem.2009.10.001](https://doi.org/10.1016/j.marchem.2009.10.001)
- Xie, H., and O. C. Zafriou. 2009. Evidence for significant photochemical production of carbon monoxide by particles in coastal and oligotrophic marine waters. *Geophys. Res. Lett.* **36**: L23606. doi:[10.1029/2009GL041158](https://doi.org/10.1029/2009GL041158)
- Xie, H., S. Bélanger, S. Demers, W. F. Vincent, and T. N. Papakyriakou. 2009. Photobiogeochemical cycling of carbon monoxide in the southeastern Beaufort Sea in spring and autumn. *Limnol. Oceanogr.* **54**: 234–249. doi:[10.4319/lo.2009.54.1.0234](https://doi.org/10.4319/lo.2009.54.1.0234)
- Zhang, Y., H. Xie, and G. Chen. 2006. Factors affecting the efficiency of carbon monoxide Photoproduction in the St. Lawrence Estuarine System (Canada). *Environ. Sci. Technol.* **40**: 7771–7777. doi:[10.1021/es0615268](https://doi.org/10.1021/es0615268)

Acknowledgments

The study was supported by an Institutional Grant (NA14OAR4170102) to the Texas Sea Grant College Program from the National Sea Grant Office as a Grants-in-Aid award to HW, National Oceanic and Atmospheric Administration, U.S. Department of Commerce. POC stable carbon isotope samples were analyzed through a prior Texas Sea Grant funded project (Award# NA14OAR4170102). We thank the Baffin Bay volunteers and the students in the Wetz lab who help the field work, Jay Brandes (Skidaway Institute Oceanography) and Chris Osburn (North Carolina State University) for providing stable isotope analyses. We also thank Z. Liu (University of Texas at Austin) for lending us the quartz bottles used in this study, and Ms. Hao Yu and Mr. Cory Saryk from TAMUCC for helping collect and analyze additional DIC samples. We also want to thank Mary and Jeff Bell Library, Division of Research and Innovation, and Office of the Provost of TAMUCC for supporting open-access publication. The authors declare that the research was conducted in the absence of any commercial or financial relationships that could be construed as a potential conflict of interest.

Submitted 14 May 2019

Revised 09 December 2019

Accepted 19 December 2019